Proton Spectra from ^{3}He + T and ^{3}He + ^{3}He Fusion at Low Center-of-Mass Energy, with Potential Implications for Solar Fusion Cross Sections

A. B. Zylstra,[1,*] J. A. Frenje,[2] M. Gatu Johnson,[2] G. M. Hale,[1] C. R. Brune,[3] A. Bacher,[4] D. T. Casey,[5] C. K. Li,[2] D. McNabb,[5] M. Paris,[1] R. D. Petrasso,[2] T. C. Sangster,[6] D. B. Sayre,[5] and F. H. Séguin[2]

[1]*Los Alamos National Laboratory, Los Alamos, New Mexico 87545, USA*
[2]*Plasma Science and Fusion Center, Massachusetts Institute of Technology, Cambridge, Massachusetts 02139, USA*
[3]*Ohio University, Athens, Ohio 45701, USA*
[4]*Indiana University, Bloomington, Indiana 47405, USA*
[5]*Lawrence Livermore National Laboratory, Livermore, California 94550, USA*
[6]*Laboratory for Laser Energetics, University of Rochester, Rochester, New York 14623, USA*

(Received 1 April 2017; revised manuscript received 7 July 2017; published 29 November 2017)

Few-body nuclear physics often relies upon phenomenological models, with new efforts at the *ab initio* theory reported recently; both need high-quality benchmark data, particularly at low center-of-mass energies. We use high-energy-density plasmas to measure the proton spectra from ^{3}He + T and ^{3}He + ^{3}He fusion. The data disagree with *R*-matrix predictions constrained by neutron spectra from T + T fusion. We present a new analysis of the ^{3}He + ^{3}He proton spectrum; these benchmarked spectral shapes should be used for interpreting low-resolution data, such as solar fusion cross-section measurements.

DOI: 10.1103/PhysRevLett.119.222701

For few-body nuclear reactions, like the fusion between three-nucleon nuclei, an *ab initio* calculation requires solving a several-body quantum system, which is challenging when including many-body forces. These many-body calculations have shown good agreement with experimental data for the $A = 5$ D + T and D + ^{3}He fusion reactions [1]. There has also been recent work [2,3] on *ab initio* structure calculations of several $A = 6$ nuclei. Typically, modeling of these reactions have relied upon *R*-matrix models [4,5], which have coefficients that must be constrained by experimental data. Reactions with three particles in the final state provide an additional challenge; the *R*-matrix theory treats the final state as sequential-decay branches, which may lack important physics of the final-state interaction of the reaction products.

A set of reactions emblematic of this challenge are the fusion reactions of ^{3}He and/or tritium (T): ^{3}He + ^{3}He, ^{3}He + T, and T + T. High-quality spectral data from accelerator-beam experiments are unavailable for these reactions, particularly ^{3}He + ^{3}He and ^{3}He + T, as reported spectra typically have poor resolution or statistics and are taken at high center-of-mass energy (E_{cm}).

The T + T reaction has been studied in accelerator-beam experiments at $E_{\mathrm{cm}} = 110$ keV [6] and at $E_{\mathrm{cm}} = 250$ keV [7]. More recently, experiments using high-energy-density (HED) plasmas measured the neutron spectrum at very low E_{cm}, 16–23 keV [8,9]. Sayre *et al.* utilize an *R*-matrix analysis to argue that the TT reaction is dominated by the ^{5}He $1/2^-$ partial wave, in contradiction to prior work. This strongly motivates studies of the ^{3}He + ^{3}He and T + ^{3}He reactions to probe the underlying physics governing the reaction of few-body systems. The T + T and ^{3}He + ^{3}He reactions are mirror reactions, expected to be governed by similar nuclear physics after Coulomb corrections.

The ^{3}He + ^{3}He reaction is of particular interest due to its role as the dominant energy-producing step in the solar proton-proton I chain [10]. The cross section (*S* factor) has been measured in several accelerator-beam experiments [11–16]. However, accurate measurements of the ^{3}He + ^{3}He produced proton spectrum have not been made at a low energy, yet it is critical for interpreting low-energy cross-section measurements relevant to solar fusion. The analysis of experimental results often assumes simple spectral shapes, such as an elliptical proton spectrum where the kinematic energy is distributed among the three reaction products assuming no nuclear interactions. The T + T mirror-reaction data suggest that this may be an inaccurate assumption.

In this Letter, we report the first measurements of charged-particle spectra from ^{3}He + ^{3}He and ^{3}He + T fusion using HED plasmas, compare the data to *R*-matrix predictions constrained by T + T data, and present new spectral shapes inferred from fits to the data. Using thermal plasmas enables high-quality measurements at low E_{cm} (86 ± 6 keV for the ^{3}He + T reaction and 165 ± 45 keV for ^{3}He + ^{3}He) of the 4π average spectrum. These reactions have the following branches:

$$^3\mathrm{He} + {}^3\mathrm{He} \rightarrow {}^4\mathrm{He} + 2p \quad (Q = 12.86\ \mathrm{MeV}) \tag{1}$$
$$\rightarrow {}^5\mathrm{Li} + p \tag{2}$$
$$\rightarrow {}^5\mathrm{Li}^* + p, \tag{3}$$
$$\mathrm{T} + {}^3\mathrm{He} \rightarrow {}^4\mathrm{He} + \mathrm{D} \quad (Q = 14.3\ \mathrm{MeV}) \tag{4}$$
$$\rightarrow {}^4\mathrm{He} + n + p \quad (Q = 12.1\ \mathrm{MeV}) \tag{5}$$
$$\rightarrow {}^5\mathrm{He} + p \tag{6}$$
$$\rightarrow {}^5\mathrm{He}^* + p \tag{7}$$
$$\rightarrow {}^5\mathrm{Li} + n \tag{8}$$
$$\rightarrow {}^5\mathrm{Li}^* + n \tag{9}$$
$$\rightarrow {}^6\mathrm{Li} + \gamma \quad (Q = 15.8\ \mathrm{MeV}) \tag{10}$$

For each reaction, the energy liberated (Q value) is given; for reactions 2 and 3, the liberated energy is equivalent to reaction 1 after the subsequent Li decay, and likewise for reactions 6–9 and 5. Measurements of the $\mathrm{T} + {}^3\mathrm{He}$ γ-ray branch [Eq. (10)] were recently reported [17]. The radiative capture reaction $^3\mathrm{He}(^3\mathrm{He}, \gamma)^6\mathrm{Be}$ has a branching ratio $\sim 4 \times 10^{-5}$ and is thus negligible [18]. In this Letter, we report measurements of the proton spectra from reactions 1–3 for $^3\mathrm{He} + {}^3\mathrm{He}$ and branches 5–9 for $\mathrm{T} + {}^3\mathrm{He}$.

The fusion reactions in this work occur in a HED plasma. The OMEGA laser [19] illuminates the outside of a thin-glass microballoon capsule filled with the gaseous fusion fuel. As the laser light is absorbed by the glass, extremely high ablation pressures develop, on the order of 100 MBar. This launches a strong spherically converging shock [20] into the gas, which rebounds at the center, creating fusion-relevant conditions in the fuel. The glass microballoon is thin enough that its mass is substantially ablated by the laser drive, an "exploding pusher" [21]. The 60 laser beams generate a total approximately 18–30 kJ of 3ω (351 nm) light in a square pulse of 0.6–1.0 ns duration [22]. An experimental schematic is shown in Fig. 1. These implosions create a fully ionized plasma approximately $80 - 100$ μm in diameter at a temperature of $\sim$20 keV and density $\sim$0.1 g/cc, with negligible [23] areal density $\lesssim 1$ mg/cm^2.

The glass capsules had thicknesses between 2 and 3 μm with diameters of $860 - 960$ μm. These capsules were diffusion filled with a mixture or T_2 and $^3\mathrm{He}$, or only with $^3\mathrm{He}$ gas, to study the two reactions of interest [24].

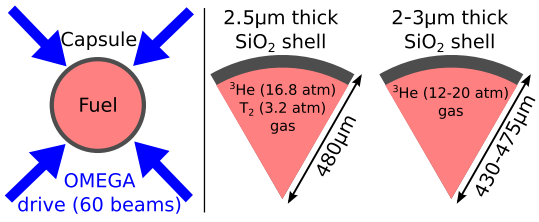

FIG. 1. Experimental schematic. Left: A capsule containing fuel is illuminated by the 60 OMEGA laser beams. Right: The capsules used in this experiment were thin-glass microballoons filled with a mixture of T_2 and $^3\mathrm{He}$ or pure $^3\mathrm{He}$.

For each study ($^3\mathrm{He} + \mathrm{T}$ or $^3\mathrm{He} + {}^3\mathrm{He}$), a set of charged-particle spectrometers based on CR-39 detection [25] were used to measure the proton spectra. For the $^3\mathrm{He} + \mathrm{T}$ study, the $\mathrm{T}^3\mathrm{He} - p$ were measured with the charged-particle spectrometers (CPS) [26] and the magnetic recoil spectrometer (MRS) [27,28]. For the $^3\mathrm{He} + {}^3\mathrm{He}$ study, the wedge range filter (WRF) spectrometers were used [29]. The CPS and MRS have better resolution ($\sim$100 keV FWHM) but less solid angle ($\sim 4 \times 10^{-6}$ [CPS] and $\sim 4 \times 10^{-5}$ [MRS] sr) and thus can be used for the $^3\mathrm{He} + \mathrm{T}$ reaction, which has a higher cross section. The WRF spectrometers can be placed within 10.5 cm of the implosion, giving a high solid angle ($\sim 3 \times 10^{-4}$ sr) for measuring products of the $^3\mathrm{He} + {}^3\mathrm{He}$ reaction, which has a much lower cross section. The WRF energy resolution is $\sim$220 keV Gaussian σ. Additionally, the WRF can measure the proton spectrum only above $\gtrsim$5 MeV.

The $^3\mathrm{He} + \mathrm{T}$ proton spectrum was measured on five OMEGA shots (70404, 70405, 70407, 70408, and 70410). To increase statistics, the individually measured spectra from each shot are summed into a single spectrum. The CPS is used for energies below 5 MeV, while the MRS is used above 5 MeV. CPS data were also taken at a higher energy, and are consistent with the MRS, but are not used due to poorer resolution at higher energy. The $^3\mathrm{He} + {}^3\mathrm{He}$ spectrum was measured on four OMEGA shots (61241, 61252, 63038, and 70411). On each shot, four WRF spectrometers are fielded, and a weighted mean spectrum is computed for each shot. Because of the low yield, the four shots are then combined into a single summed spectrum to improve statistics (see Supplemental Material [30]). The WRFs can measure the spectrum only at higher energies.

The average E_{cm} for each reaction must also be known. Fuel ion temperatures are typically diagnosed by spectroscopy of Doppler-broadened fusion-product lines. Since the fuel contains a small impurity of deuterium (D), we use the $^3\mathrm{He}(\mathrm{D}, p)^4\mathrm{He}$ reaction as a temperature diagnostic by measuring the proton line width. The fuel temperature is inferred using relativistic kinematics [31]. For the $^3\mathrm{He} + \mathrm{T}$ reaction the temperature dependence is very similar to $^3\mathrm{He} + \mathrm{D}$, so E_{cm} was determined to be 86 ± 6 keV for the $^3\mathrm{He} + \mathrm{T}$ data. For the $^3\mathrm{He} + {}^3\mathrm{He}$ reaction, the $^3\mathrm{He} + \mathrm{D}$ burn-averaged temperature is taken as a lower limit, with an upper limit from radiation-hydrodynamics calculations, giving $E_{\mathrm{cm}} = 165 \pm 45$ keV. For more discussion on determining E_{cm}, see Refs. [17,32,33].

R-matrix modeling [4,5,34], which is a phenomenological treatment based on several "feeding factors" related to scattering amplitudes and the relative abundance of reaction branches, was used to predict the spectral components for these nuclear reactions. The feeding factors were determined from a fit to the Wong, Anderson, and McClure (Ref. [7]) $\mathrm{T} + \mathrm{T}$ data at $E_{\mathrm{cm}} = 250$ keV. The calculation accounts for the difference in reactants by the basic mirror symmetry assumption.

The calculated R-matrix proton spectra are shown in Figs. 2(a) (^{3}He + ^{3}He) and 2(b) (T + ^{3}He). The dashed curves result from the calculations constrained by the Wong, Anderson, and McClure T + T data. The total proton spectrum (black curve) results from the contributions of several branches of the reaction. For ^{3}He + ^{3}He, the branches are ^{4}He + pp (diproton, magenta curve) and through sequential decay of a proton plus ^{5}Li in the ground state (red curve) or an excited state (blue curve). The diproton branch represents 27% of the total, while the ground and excited states of ^{5}Li are 21% and 51%, respectively. For ^{3}He + T the reaction branches are ^{4}He + n + p (magenta [18.4%]), proton emission and sequential decay through ^{5}He in the ground state or excited state (red [11.1%] and blue [25.8%], respectively), or neutron emission and sequential decay through ^{5}Li in the ground or excited state (green [9.7%] and cyan [35%], respectively). The calculated spectra are shown area normalized to 1.

Our calculated spectra do not have a component with an elliptical shape, which is a common approximation in the literature. This would result from having uncharged particles with angular momentum $\ell = 0$ in all coordinates. Since most of the resonances have $\ell = 1$, and the particles are charged, the closest thing we have to this shape are the magenta curves corresponding to the S-wave dinucleon resonances ($p - p$ and $n - p$ for ^{3}He + ^{3}He and ^{3}He + T, respectively). A purely elliptical shape does not arise in any natural way from the theory, nor would it appear to improve the agreement between the data and our calculations.

To compare with the data, the calculated Wong R-matrix spectrum is convolved with a thermal Doppler width and the instrument response function [35]. The total particle yield is then set by a χ^2 minimization, adjusting only the overall amplitude to best match the data. The comparison is shown in Figs. 2(c) (^{3}He + ^{3}He) and 2(d) (^{3}He + T), where the blue points are the data and the red dashed curves are the convolved R-matrix predicted proton spectra.

The data show some significant discrepancies with the R-matrix calculations. For the ^{3}He + ^{3}He reaction, the fit clearly overestimates the spectral amplitude between ~7 and 8.5 MeV when matching the peak at 9.2 MeV that corresponds to the ^{5}Li ground state [see Fig. 2(c)]. For the ^{3}He + T reaction, the calculation clearly underestimates the strength of the ^{5}He ground state, missing the amplitude of

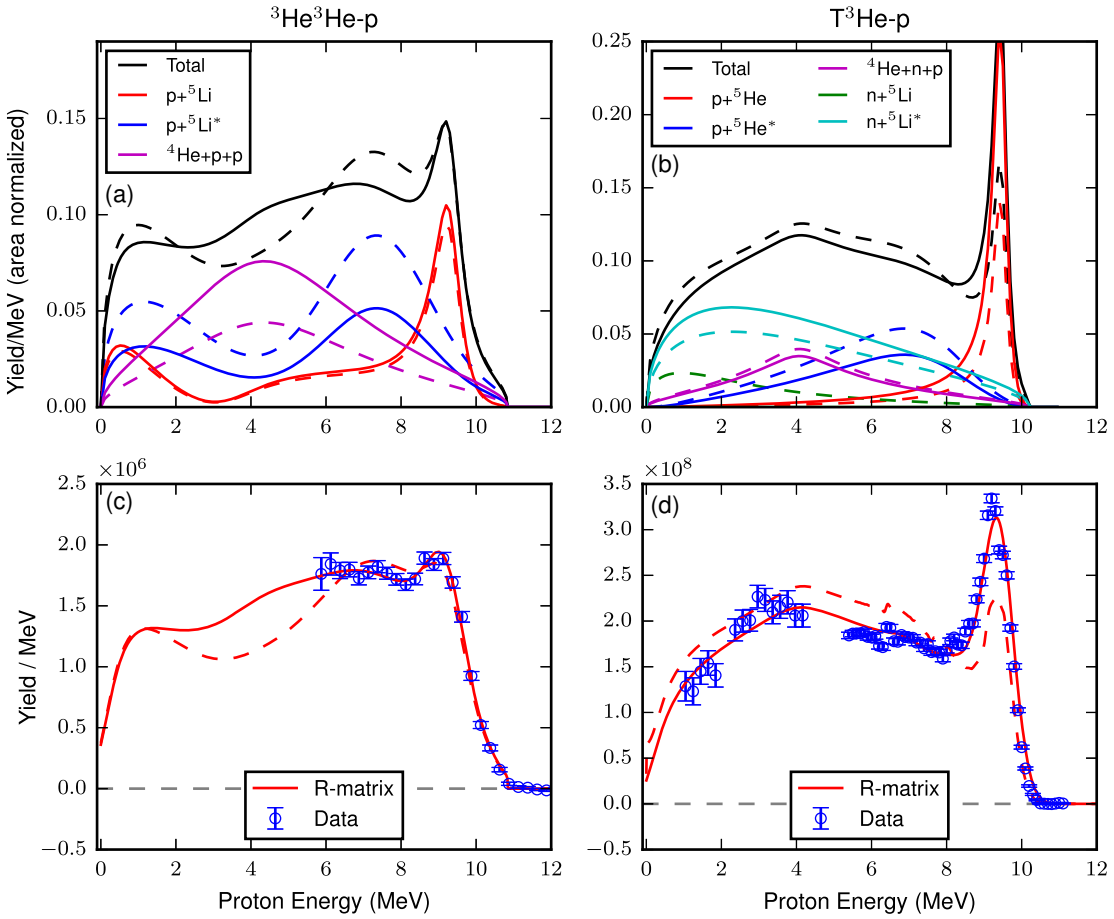

FIG. 2. Top row: R-matrix calculations of the total proton spectrum and components for ^{3}He + ^{3}He (a) and ^{3}He + T (b). Bottom row: Comparison of the calculated R-matrix spectrum to the data for ^{3}He + ^{3}He (c) and ^{3}He + T (d). Dashed curves are using feeding factors from the Wong, Anderson, and McClure data, and solid curves are from the fit to our data.

the peak at 9 MeV by about 40%, while overestimating the prevalence of the remaining components. These differences are likely a result of the R-matrix amplitudes (feeding factors) not being the same for the ^{6}Li (T + ^{3}He) and ^{6}Be (^{3}He + ^{3}He) systems as they are for the ^{6}He (T + T) system to which they were fit. There is also the possibility of an energy dependence in these amplitudes that was not taken into account, since the Wong experiment was at higher E_{cm}.

To better explain the data, we fit the spectral data varying the prevalence of each reaction branch; the best-fit results are shown in Fig. 2 by the solid curves. For the ^{3}He + ^{3}He data, the $p + {}^5$Li ground state is slightly increased to $(24 \pm 1_{stat} \pm 2_{sts})\%$, the $p + {}^5$Li* branch is substantially reduced to $(29 \pm 3_{stat} \pm 3_{sts})\%$, and the $pp + {}^4$He branch is increased to $(46 \pm 5_{stat} \pm 6_{sts})\%$. We quote uncertainties from both a statistical component as well as uncertainty due to shot-to-shot variation in the spectral shape, which are independent sources of uncertainty (see Supplemental Material [30]). As shown in Fig. 2(c), the quality of fit is much improved; the reduced χ^2 is 1.6 versus 3.9 for the Wong-constrained spectrum. For the ^{3}He + T proton spectrum, the $p + {}^5$He branch is approximately doubled to 20%, while the other branches are reduced. The agreement with the ^{5}He ground state is significantly improved. The best fit is also in reasonable agreement with the data between 1 and 4 MeV, given the statistical uncertainty in the data, where the shape is primarily dictated by the $n + {}^5$Li* and ^{4}He + n + p branches. For more discussion of the best fits to both spectra, see Supplemental Material [30].

A second R-matrix calculation was performed for the ^{3}He + ^{3}He reaction. In this second model, the R-matrix calculation was first constrained by lower-energy TT-n data from the national ignition facility (NIF) [9], included an angular effect in the exchange amplitudes, and included the $1/2^+$ S-wave channel. For details of the model differences, see Ref. [36]. A comparison of these two models is shown in Fig. 3. The top plot (a) shows the total spectrum from each calculation. To compare with the data, each model is convolved with the thermal Doppler broadening and detector response function (b). The second model seems to further underestimate the ^{5}Li ground state, shown by the clear disagreement with the data around 9 MeV. The dashed curves for each model use feeding factors from the T + T data (Refs. [7,9], respectively). We also perform a fit of our data using model 2, which requires a 1.77× increase in the feeding factor for the ^{5}Li ground state relative to Ref. [9], which is shown in Fig. 3 by the solid curves.

While both models describe the measured ^{3}He + ^{3}He proton spectrum well, a significant difference in shape exists at a low energy. This results in the inferred proton yield, integrated over the whole spectrum, differing by 5% between these models. Using the T + T predicted spectra or simple models can result in larger deviations in the inferred yield, up to ∼10%. In any experiments that must assume a spectral shape, such as low-resolution or low-statistics accelerator measurements, we recommend that these best-fit spectra be used until a better understanding can be reached and include a corresponding uncertainty in the spectrum bounded by our two models. This could potentially contribute to uncertainty in the ^{3}He + ^{3}He cross section at solar-fusion-relevant energies.

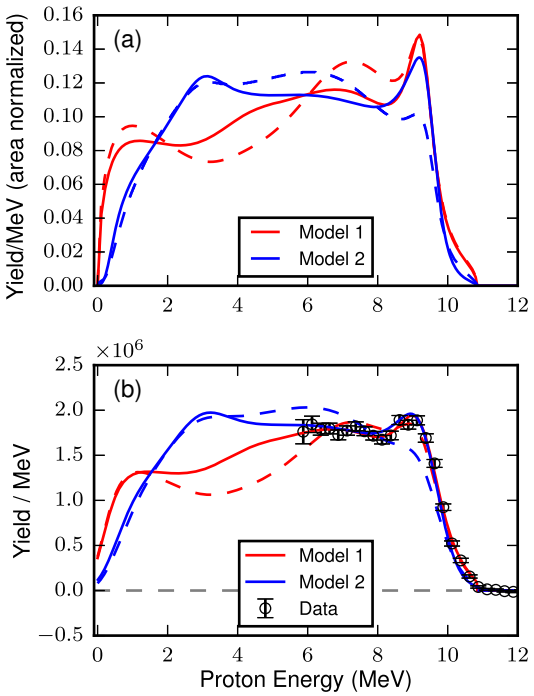

FIG. 3. Second R-matrix calculation for ^{3}He + ^{3}He (model 2) constrained using lower-energy TT data. (a) Comparison of the total spectrum (area normalized). (b) Comparison of each model to the data. For each model, the dashed curve is as predicted using T + T data in the literature, and the solid curve is the best fit to our data.

In conclusion, the first measurements of proton spectra from the $A = 6$ fusion reactions ^{3}He + ^{3}He and ^{3}He + T using inertial fusion implosions are reported in this Letter. This relatively new measurement technique using a thermal plasma as the source has been used in several recent works [8,9,17,33], notably for new measurements of the T + T fusion neutron spectrum at lower energies than were possible in accelerator-beam experiments. This work complements those results by studying the reactions ^{3}He + ^{3}He and ^{3}He + T, measuring high-fidelity spectra at a low energy for the first time. We compare the data to predicted spectra from new R-matrix calculations that were constrained by TT-n data higher or lower energy and find significant disagreement. This suggests that there is either an unexpected difference between these reactions that is not accounted for in the R-matrix calculations or a strongly energy-dependent mechanism. Within each framework, we report a new analysis of the ^{3}He + ^{3}He proton spectrum based on best fits to our data. In addition to the relevance of this work to basic nuclear physics, the spectral shape of ^{3}He + ^{3}He at a low energy is particularly important in the

inference of that reaction's cross section from low-statistics accelerator-beam experiments.

These data provide a strong constraint on future theory work, either using *ab initio* techniques or the *R*-matrix method. An even stronger constraint than these data could be provided by measurements of the low-energy part of the ^{3}He + ^{3}He spectrum, particularly between 1 and 5 MeV [see Fig. 3(b)], where we find substantial differences between the two models. This work is also significant in that it is the first measurement of the ^{3}He + ^{3}He fusion reaction in a plasma environment. Experiments at laser facilities, such as OMEGA and the NIF, can provide a plasma environment similar to astrophysical systems like stellar cores and the Universe during big-bang nucleosynthesis [17,33]. This work therefore opens up further studies of the spectrum closer to stellar energies and measurements of the ^{3}He + ^{3}He cross section in a plasma environment.

We thank the operations crews and engineering staff at OMEGA for supporting these experiments and E. Doeg and R. Frankel for their work processing the CR-39. This work was supported in part by the U.S. DOE (Grants No. DE-NA0001857, No. DE-FC52-08NA28752, No. DE-FG02-88ER40387, No. DE-NA0001837, and No. DE-AC52-06NA25396), LLNL (No. B597367), LLE (No. 415935-G), the Fusion Science Center at the University of Rochester (No. 524431), and the National Laser Users Facility (No. DE-NA0002035). A. B. Z. acknowledges support by the National Science Foundation Graduate Research Fellowship Program under Grant No. 1122374 and gratefully acknowledges the support provided for this work by the Laboratory Directed Research and Development (LDRD) program, Project No. 20150717PRD2, at Los Alamos National Laboratory.

*zylstra@lanl.gov

[1] P. Navrátil and S. Quaglioni, Phys. Rev. Lett. **108**, 042503 (2012).
[2] C. Romero-Redondo, S. Quaglioni, P. Navrátil, and G. Hupin, Phys. Rev. Lett. **113**, 032503 (2014).
[3] G. Hupin, S. Quaglioni, and P. Navrátil, Phys. Rev. Lett. **114**, 212502 (2015).
[4] A. M. Lane and R. G. Thomas, Rev. Mod. Phys. **30**, 257 (1958).
[5] F. Barker, Aust. J. Phys. **41**, 743 (1988).
[6] K. W. Allen, E. Almqvist, J. T. Dewan, T. P. Pepper, and J. H. Sanders, Phys. Rev. **82**, 262 (1951).
[7] C. Wong, J. Anderson, and J. McClure, Nucl. Phys. **71**, 106 (1965).
[8] D. T. Casey *et al.*, Phys. Rev. Lett. **109**, 025003 (2012).
[9] D. B. Sayre *et al.*, Phys. Rev. Lett. **111**, 052501 (2013).
[10] H. A. Bethe, Phys. Rev. **55**, 434 (1939).
[11] M. R. Dwarakanath and H. Winkler, Phys. Rev. C **4**, 1532 (1971).
[12] A. Krauss, H. Becker, H. Trautvetter, and C. Rolfs, Nucl. Phys. **A467**, 273 (1987).
[13] C. Arpesella *et al.*, Phys. Lett. B **389**, 452 (1996).
[14] M. Junker *et al.* (LUNA Collaboration), Phys. Rev. C **57**, 2700 (1998).
[15] R. Bonetti *et al.* (LUNA Collaboration), Phys. Rev. Lett. **82**, 5205 (1999).
[16] N. Kudomi, M. Komori, K. Takahisa, S. Yoshida, K. Kume, H. Ohsumi, and T. Itahashi, Phys. Rev. C **69**, 015802 (2004).
[17] A. B. Zylstra *et al.*, Phys. Rev. Lett. **117**, 035002 (2016).
[18] W. Harrison, W. Stephens, T. Tombrello, and H. Winkler, Phys. Rev. **160**, 752 (1967).
[19] T. Boehly *et al.*, Opt. Commun. **133**, 495 (1997).
[20] G. Guderley, Luftfahrtforschung **19**, 302 (1942).
[21] M. D. Rosen and J. H. Nuckolls, Phys. Fluids **22**, 1393 (1979).
[22] Truncation of the laser pulse was not found to affect the nuclear performance, as the end of the drive does not efficiently couple energy to the shock-heated fuel in these exploding pushers.
[23] The charged fusion products can be slowed by material (primarily the plasma electrons); however, for small areal densities (1 mg/cm^2 or less) the energy shift is small ($\lesssim$50 keV). This is confirmed by the fact that several spectral lines (D^{3}He-p and the ^{5}He and ^{5}Li ground states) are measured at their known birth energy within the experimental uncertainties.
[24] The T_2 gas supply used was contaminated with approximately 1.5% atomic D. Similarly, the ^{3}He supply is contaminated with approximately 0.01% D. The ^{3}He-rich mixture (72% atomic ^{3}He) was chosen for the mixed fill to increase the S/B for a separate γ measurement [17] on these shots, as the primary source of background for that measurement comes from the T(D, γ)^{5}He reaction. Even with the low D contamination level, the much higher cross section for D + T fusion results in a large number of reactions.
[25] F. H. Séguin *et al.*, Rev. Sci. Instrum. **74**, 975 (2003).
[26] D. Hicks, Ph.D. thesis, Massachusetts Institute of Technology, 1999.
[27] J. Frenje *et al.*, Rev. Sci. Instrum. **79**, 10E502 (2008).
[28] D. T. Casey, Ph.D. thesis, Massachusetts Institute of Technology, 2012.
[29] F. H. Séguin *et al.*, Rev. Sci. Instrum. **83**, 10D908 (2012).
[30] See Supplemental Material at http://link.aps.org/supplemental/10.1103/PhysRevLett.119.222701 for a detailed discussion of the spectral analysis and fits, plus tabulated values of our best-fit spectra.
[31] L. Ballabio, J. Källne, and G. Gorini, Nucl. Fusion **38**, 1723 (1998).
[32] A. B. Zylstra, Ph.D. thesis, Massachusetts Institute of Technology, 2015.
[33] M. Gatu Johnson *et al.*, Phys. Plasmas **24**, 041407 (2017).
[34] M. W. Paris and G. M. Hale, *EPJ Web Conf.* 122, 08002 (2016).
[35] For the WRF proton spectrometer, the instrument response is a 220 keV (σ) Gaussian function [29]. The CPS spectrometer has a "boxcar" response with an energy-dependent width [26]. For the MRS spectrometer, a Monte Carlo calculated response matrix is used [27,28].
[36] C. R. Brune, J. A. Caggiano, D. B. Sayre, A. D. Bacher, G. M. Hale, and M. W. Paris, Phys. Rev. C **92**, 014003 (2015).